The effect of mode excitations on the absorption enhancement for silicon thin film solar cells

Albert Lin, Yan-Kai Zhong, and Ssu-Ming Fu

Citation: Journal of Applied Physics **114**, 233104 (2013); doi: 10.1063/1.4851817
View online: http://dx.doi.org/10.1063/1.4851817
View Table of Contents: http://scitation.aip.org/content/aip/journal/jap/114/23?ver=pdfcov
Published by the AIP Publishing

The effect of mode excitations on the absorption enhancement for silicon thin film solar cells

Albert Lin,[a] Yan-Kai Zhong, and Ssu-Ming Fu
Department of Electronic Engineering, National Chiao-Tung University, Hsinchu 30010, Taiwan

(Received 6 September 2013; accepted 5 December 2013; published online 19 December 2013)

Periodic gratings on solar cell back reflectors are an alternative to randomly textured surfaces to provide absorption enhancement. Theoretically, it is impossible to excite quasi-guided modes at every wavelength for a given grating geometry and the broad band enhancement can only be achieved by strong absorption peaks at several wavelengths. Therefore, the critical issue is how to maximize the short circuit current using a limited number of discrete quasi-guided modes. In this work, a common dielectric-semiconductor-dielectric-metal solar cell structure is investigated. It is found that although the number of guided mode peaks has pronounced effect on the solar cell short circuit current, the geometry resulting in the highest short circuit current does not coincide with the geometry leading to the most supported modes. It is also found that high-Q modes are always resulted from global optimization for TE incidence, while low-Q modes are resulted for TM incidence on one-dimensional gratings without a dielectric spacer. Besides, a properly designed and configured dielectric spacer can provide >40% improvement in short circuit current. It is therefore suggested for solar cells with metallic back reflectors, dielectric spacer should be included, and the texture should be formed on the dielectric spacer itself rather than on the metal. Finally, the optimization of the mode quality is proved to be critical in all cases, in addition to the number of supported modes. © *2013 AIP Publishing LLC*. [http://dx.doi.org/10.1063/1.4851817]

I. INTRODUCTION

Periodic grating can enhance solar cell absorbance by providing quasi-guided mode excitations.[1–14] Nonetheless, quasi-guided modes cannot exist over the entire solar spectrum due to its discrete nature. The question arises: How to utilize the limited-number, non-continuous qausi-guided modes to maximize the short circuit current. Previously, it has been assumed that the broad band absorbance enhancement is proportional to the number of guided mode peaks.[4,8] The work from the same authors later proposes a distinction to the mode quality in terms of its overlap-integral.[15] More recent experimental work studies the dispersion and the absorption enhancement, and motivates the concept that mode confinement, i.e., Q-factor, also plays an important role in determining the broad band absorbance.[3] It is also interesting to know whether it is more efficient to use narrow band high-Q peaks or to use fewer broad band low-Q peaks, to cover a specific spectral range. In this work, it is shown that while the number of guided mode peaks has pronounced effect on the short circuit current, other factors such as the mode quality and the mode excitation wavelength and strength also affect the short circuit current. This leads to the observation that the solar cell geometry giving the most guided modes does not coincide with the geometry giving the highest short circuit current. In this work, the solar cell geometry is optimized using global optimization algorithm[16] to maximize the short circuit current at light trapping wavelength($J_{SC,LT}$), and the resulting spectral response is analyzed and compared. The investigation is conducted for the absorption enhancement for TE and TM incidence, respectively, since only TM incidence can excite surface plasmons for one-dimensional (1D) gratings in two-dimensional (2D) simulation domain if there is no dielectric spacer. The optimization is repeated for several runs to confirm the result, and very similar conclusion is arrived. For TE incidence, it is found that the modes are mostly of diffractive nature. The excited modes exhibit high-Q resonance and the air-dielectric-semiconductor-metal essentially acts as a conventional index-guided waveguiding structure. On the other hand, surface plasmon (SP) has long been known for its broad band emission[6,7,9–12,14] capability. According to the study here, the quasi-guided modes associated TM incidence on 1D gratings without a dielectric spacer exhibit low-Q broad band resonances and the absorbance enhancement is mostly through the broad band coverage of solar spectrum. This is pronouncedly different from the high-Q diffractive modes for TE incidence.

II. GEOMETRY AND PROBLEM SET-UP

In this work, the discretization of Maxwell's equation is carried out by two-dimensional finite element method, using COMSOL Multiphysics software package.[17] Periodic boundary conditions are set at the left and right boundaries, while perfectly matched layer absorbing boundary conditions are used at the top and bottom boundaries of the computational domain. The p-i-n diode structure is assumed and 20 nm thick p and n layers are used here, which is a common thickness for experimental thin-film silicon solar cells. The absorbance in i-silicon is then calculated by integrating the divergence of the time-averaged Poynting vector, which is then normalized by the incident power. Only absorbance in

[a]hdtd5746@gmail.com

silicon generates electron-hole, while the absorbance in metal leads to absorption loss. In addition, only the electron-hole pairs generated in i-layer will be collected. The details of the calculation can be found in Refs. 13 and 17–20. The absorbance is calculated by integrating the power dissipation in intrinsic silicon layer

$$A(\lambda) = \frac{\frac{1}{2}\int_V \omega\varepsilon_0\varepsilon''(\lambda)|\vec{E}(\vec{r})|^2 dv}{\frac{1}{2}\int_S \mathrm{Re}\left\{\vec{E}(\vec{r}) \times \vec{H}^*(\vec{r})\right\} \cdot d\vec{s}}, \quad (1)$$

where ω is the angular frequency, λ is the free space wavelength, ε_0 is the permittivity in vacuum, and ε'' is the imaginary part of complex semiconductor dielectric constant. The short circuit current at light trapping wavelength, $J_{SC,LT}$(600 nm–1000nm) is calculated by averaging $A(\lambda)$ weighted by AM 1.5 solar spectrum

$$J_{SC,LT} = q\int \frac{\lambda}{hc}\Omega(\lambda)A(\lambda)d\lambda, \quad (2)$$

where $\Omega(\lambda)$ is AM 1.5 solar spectrum in unit of J s^{-1} cm^{-2} nm^{-1}, h is the Plank constant, λ is the free space wavelength, q is the elementary charge, and c is the speed of light in vacuum. The genetic algorithm is chosen as the global optimization techniques for locating the optimized geometry for the periodic grating on the solar cell back reflector. It is chosen due to the fact that the genetic algorithm has been proved to be very effective in different engineering fields.[21–24] During the optimization procedure, the objective function is defined as the short circuit current at light trapping wavelength ($J_{SC,LT}$), which is to be maximized by adjusting grating geometry. The objective value will keep increasing and then saturate, as the optimization goes on. When the optimization runs for long enough time, the objective value will gradually converge to the global maximum of the objective function. In order to reveal the relationship between the number of supported quasi-guided modes and $J_{SC,LT}$, the number of qausi-guided modes for each individual (sample) is monitored during the optimization procedure. To strengthen the conclusion, several optimization runs are conducted and highly similar result and observation are arrived, and these results are included in Secs. III and IV.

The first structure under study is a silver back reflector directly in contact with silicon with a 1D grating in 2D simulation domain. Both TE and TM polarizations are used to study the respective quasi-guided mode excitations, as illustrated in Fig. 1. Using TM polarization in 2D simulation domain to study the plasmonic structures has been employed in literature.[2,25] Afterward, the effect of dielectric spacer is studied to reveal the effect of dielectric shielding on the surface plasmonic absorption, for TM polarization. It should be noted that surface plasmon polaritons (SPP) can only be excited for TM incidence on 1D gratings without a dielectric spacer, while TE polarized light cannot.[2,25] In addition, the inclusion of a dielectric spacer in general eliminates the possibility of SPP excitations and therefore can reduce metallic absorption loss.

The study is arranged as follows: First, the relationship between quasi-guided modes and absorption enhancement is conducted, for TE incidence and TM incidence on a 1D grating without a dielectric spacer, respectively. Afterward, the usage of dielectric spacers on mitigating surface plasmon absorption and its effect on the optimal quasi-guided mode excitations are assessed for TM polarized light. For the generalization to solar cells in three-dimensional (3D) domain, the TE incidence is more related to the solar cells with dielectric mirrors where all of the excited modes are of purely diffractive nature. For TM incidence, it is more related to thin-film solar cells with 2D-textrued or 2D-grated metallic back reflectors. For 2D metallic texturing/grating in 3D domain, if there is no dielectric spacer, the excitation of SPP is possible for both polarizations. As a result, the SP absorption has to be mitigated by a dielectric spacer for both polarizations.

The film thickness is 0.3 μm and poly crystalline silicon (poly Si) is used as an example to study different solar cell structures. For experimental poly Si thin-film solar cell, the typical thickness is 1–2 μm. Here, the thickness is kept thinner than full absorption to better reflect the light trapping effect. This is similar to Yu *et al.*[8] where 3 μm crystalline silicon is used for weak absorption, while full absorption thickness of c-Si solar cells is around 200 μm. It should be emphasized that the conclusions drawn here do not only apply to poly crystalline silicon but also apply to other inorganic semiconductors as well. This is due to the similar mode coupling, light scattering, and waveguiding behaviors in inorganic solar cells. Crystalline silicon parameters have also been tested and the conclusion is the same except slightly lower short circuit current values. For organic solar cells, the near field enhancement is more dominant and the conclusions here may not apply. The wavelength range chosen is from 600 nm to 1000 nm which corresponds to the long-wavelength light trapping regime for silicon solar cells where the quasi-guided mode excitation is critical. The material refractive index and extinction coefficient is from Rsoft material database[26] and literature.[27–32] The central processing unit (CPU) runtime

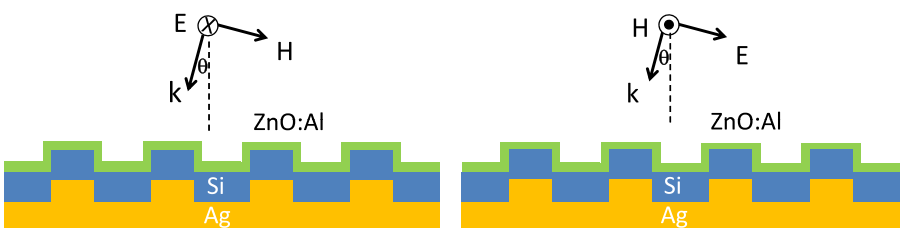

FIG. 1. The set-up for investigating TE incidence and TM incidence on one-dimensional gratings in two-dimensional space.

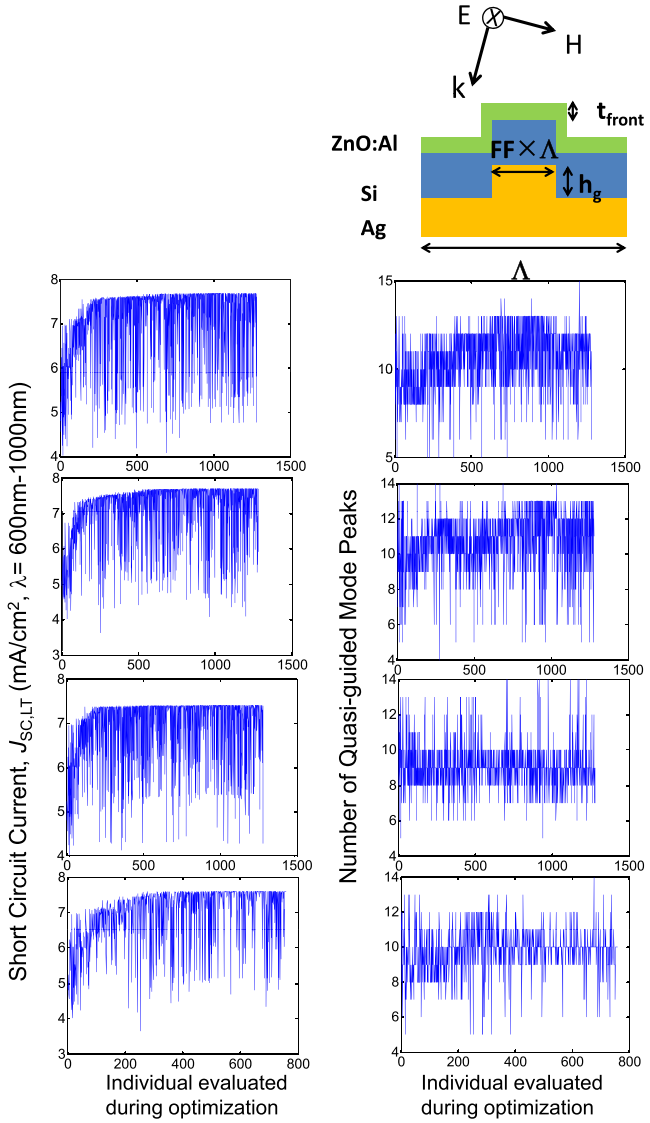

FIG. 2. The statistics of global optimization for TE diffractive absorption enhancement. (Left) Evolution of the short circuit current as the optimization proceeds. (Right) Evolution of the number of quasi-guided mode peaks as the optimization proceeds.

for a single optimization run is around 72 h using Intel quad-core Xeon 3.1 GHz processor. It is worth mention that 1D grating or texture is in 2D simulation domain, and 2D grating or texture is in 3D simulation domain. In the paragraph below, when 1D or 2D grating is mentioned, the specification of the simulation domain may be omitted but its meaning should be clear from the explanation above.

III. ABSORPTION ENHANCEMENT FOR TE INCIDENCE WITHOUT A DIELECTRIC SPACER

The optimized geometry for the highest short circuit current at light trapping wavelength ($J_{SC,LT}$) is $\Lambda = 0.5\,\mu$m, fill factor (FF) = 0.24, hg = 0.07 μm, and $\theta = 12.91°$ for the absorption enhancement at TE incidence. The front ZnO:Al thickness(t_{front}) is 80 nm, which is a common thickness value for experimental thin-film silicon solar cells. The same front ZnO:Al thickness is used for other studies in this paper. The optimized highest short circuit current at light trapping wavelength ($J_{SC,LT}$) is 7.69 mA/cm^2 with respect to AM1.5 spectrum. The evolution of the number of quasi-guided modes and the short circuit current at light trapping wavelength ($J_{SC,LT}$) is plotted in Fig. 2, and the spectral response is plotted in Fig. 3. From Fig. 2, it is observed that $J_{SC,LT}$ increases monotonically. The monotonically increased $J_{SC,LT}$ with optimization is trivial since $J_{SC,LT}$ is defined as the objective function during the optimization. The number of quasi-guided modes also increases with the optimization but it has overshoots during optimization. The increased number of the quasi-guided modes during optimization indicates that the number of supported modes indeed has a significant effect on solar cell absorbance. Nevertheless, the overshoots imply that the structure supports the most modes might not lead to the highest $J_{SC,LT}$. This point becomes clearer by plotting the spectral response of the highest $J_{SC,LT}$ individual and the most guided mode peak individual during optimization in Fig. 3. In the left of Fig. 3, the optimal individual is plotted. If the optimization is effective, this is the highest $J_{SC,LT}$ geometry, but its supported guided modes are less than the spectral response at the right of Fig. 3, which is

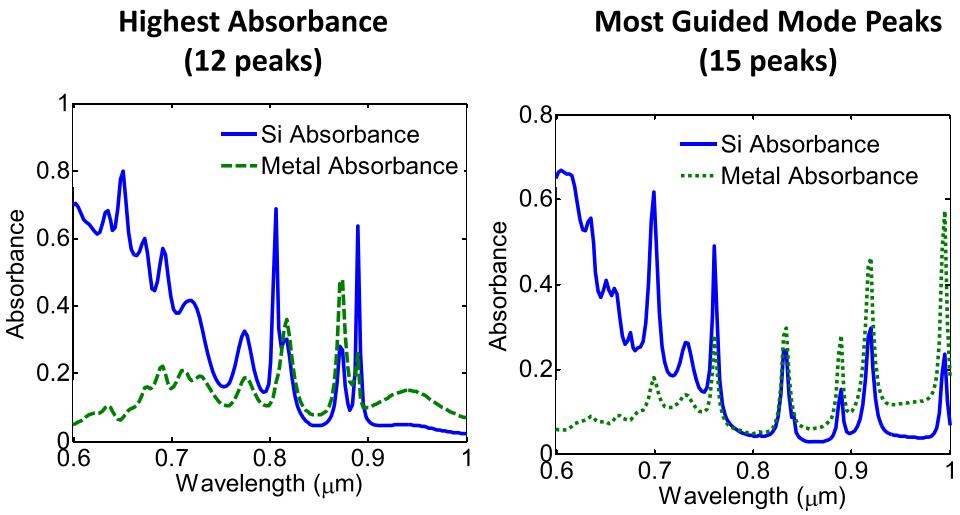

FIG. 3. The spectral absorbance of the silicon film for TE incidence after optimization with respect to short circuit current at light trapping wavelength. (Left) The spectral response for the highest short circuit current. (Right) The spectral response for the most quasi-guided modes peaks during optimization.

a structure supporting more modes. In fact, the most guided mode geometry is an individual that the optimization procedure has been going through (evaluated) but not converged into. This indicates that the number of modes is not the solely concern for high short circuit current. As a result, the conclusion can be drawn that the optimized geometry that gives the highest $J_{SC,LT}$ does not coincides with the geometry that leads to the most quasi-guided mode excitations, and the optimization of the mode quality factor(Q-factor) is essential. The optimized incident angle is slightly deviated from the normal direction, consistent with the previous study.[25] In a general trend, $J_{SC,LT}$ decreases with the incident angle since the effective incident power coupled into the solar cell is scaled with $\cos\theta$ along the line of geometrical optics. This is also easily conceivable from elementary earth sciences. Nonetheless, oblique incidence is beneficial for photon in-coupling into the Bloch propagation guided modes, and the joint effect results in that the optimal angle slightly deviates from the normal incidence where the optimal balance between effective incident power and Bloch waveguiding is achieved. From the spectral response in Fig. 3, it is observed that high-Q diffractive resonance is resulted for the optimized geometry for the highest $J_{SC,LT}$. This indicates that for the TE incidence, the most effective way to utilize diffraction and index-guiding is managing to attain narrow band absorption peaks within the spectral range of interest. This point will become even clearer in Sec. IV where the optimized spectral response for the TM incidence on 1D gratings without a dielectric spacer is shown for comparison. In reality, only dielectric mirror can completely eliminate SP absorption, such as distributed brag reflector (DBR) backed solar cell. This is due to the fact that for real metallic back reflectors, the texture or grating is most of the time two-dimensional rather than one-dimensional, and the surface plasmon absorption exists for both TE and TM polarization. It is found here that due to no SP absorption, TE incidence on a 1D grating here can provide higher $J_{SC,LT}$, compared to the $J_{SC,LT}$ values of TM incidences with or without a dielectric spacer. The results for TM incidence will be revealed later in Secs. IV and V. Based on this observation, purely diffractive back reflectors such as dielectric mirrors can potentially replace the conventional metallic back reflectors for higher $J_{SC,LT}$.

IV. ABSORPTION ENHANCEMENT FOR TM INCIDENCE WITHOUT A DIELECTRIC SPACER

The optimized geometry for TM incidence without a dielectric spacer, with the objective function defined as short circuit current at light trapping wavelength ($J_{SC,LT}$), is $\Lambda = 0.55\,\mu$m, FF = 0.31, hg = 0.06 μm, and $\theta = 7.24°$. t_{front} is fixed at 80 nm. The optimized highest short circuit current at light trapping wavelength ($J_{SC,LT}$) is only 4.77 mA/cm^2 with respect to AM1.5 spectrum. Similar to the previous study for the TE diffractive quasi-guided modes, the evolution for the number of quasi-guided modes and the evolution of the short circuit current at light trapping wavelength ($J_{SC,LT}$) is plotted in Fig. 4. During the optimization, the samples with higher short circuit current are searched and therefore the short

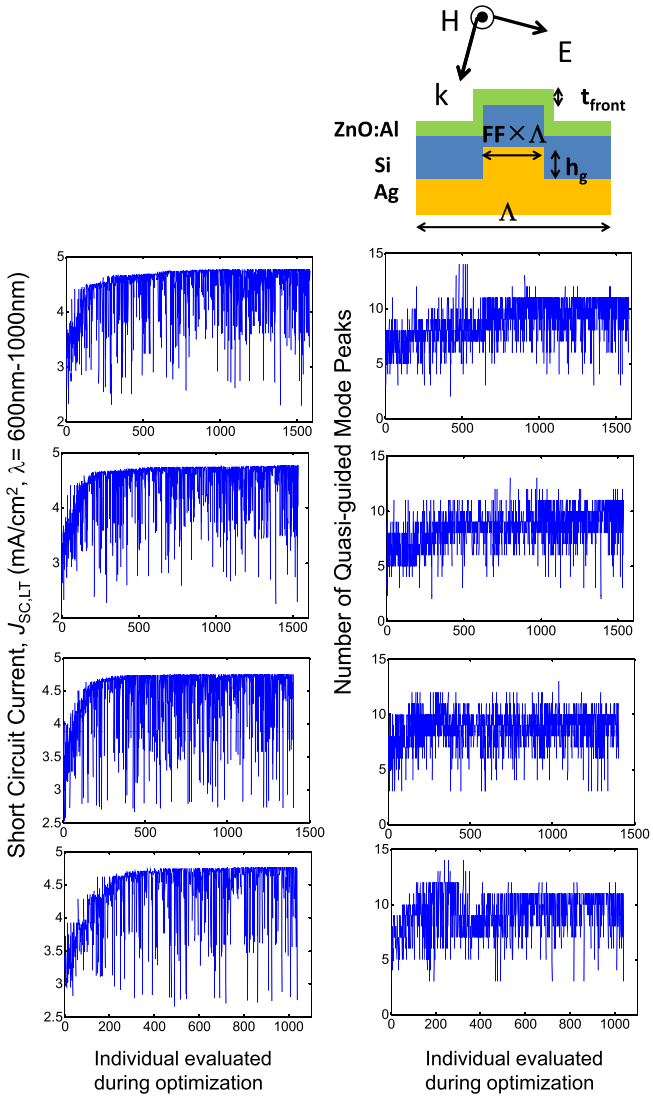

FIG. 4. The statistics of global optimization for the absorption enhancement for TM incidence without a dielectric spacer. (Left) Evolution of short circuit current as the optimization proceeds. (Right) Evolution of the number of quasi-guided mode peaks as the optimization proceeds.

circuit current values show monotonic increase as illustrated in Fig. 4. On the other hand, the number of quasi-guided modes also shows significant overshoots during optimization. As a result, for the absorption enhancement for TM incidence, it is also found that the geometry leading to the highest $J_{SC,LT}$ does not coincide with the geometry giving the most quasi-guided modes. What is different from the previous TE incidence is that now the quasi-guided modes are not of diffractive nature. From Fig. 5, the spectral response shows several low-Q resonance peaks, which can be attributed to the broad band nature of the surface plasmon excitation at the metal-semiconductor interface. Surface plasmon has long been known to be capable of broad band emission[6,7,9–12,14] and as far as the broad band solar cell application is concerned, this might promote photon absorption at broader bandwidth if the metallic absorption is properly reduced. The optimization on the grating geometry here confirms that for the absorption enhancement for TM incidence on 1D gratings without a dielectric spacer, the most

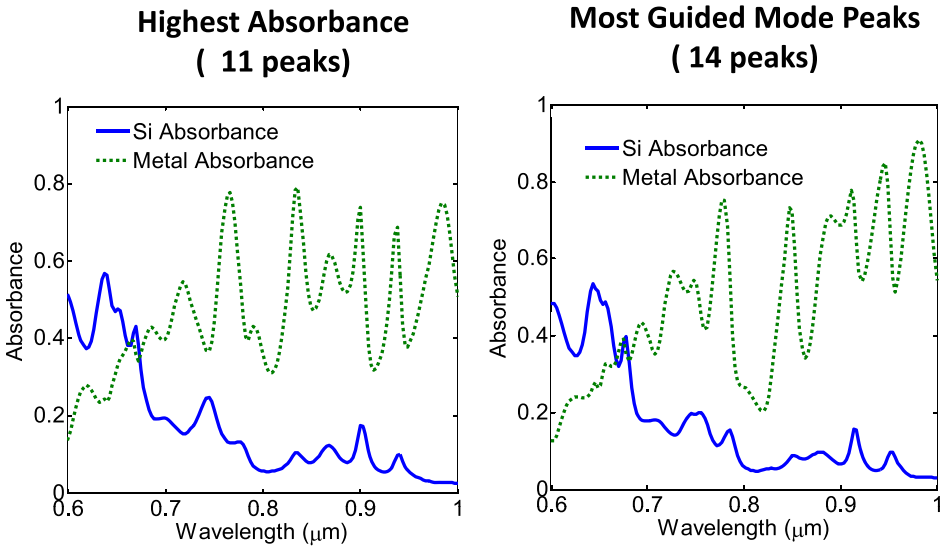

FIG. 5. The spectral absorbance of the silicon film for TM incidence without a dielectric spacer, after optimization with respect to short circuit current at light trapping wavelength. (Left) The spectral response for the highest short circuit current. (Right) The spectral response for the most quasi-guided modes peaks during optimization.

efficient way to trap the solar photons is using broad band low-Q resonance peaks. From Fig. 5, the metallic absorption loss is significant for TM incidence on 1D gratings without a dielectric spacer due to SP excitations, especially at the long wavelength portion of solar spectrum. While the metallic absorption is inevitable as long as a metallic back reflector is employed, it should be mitigated, possibly by a dielectric spacer, in order to better utilize the advantage associated with the plasmonic photovoltaics. For solar cells with 2D texture or 2D grating in 3D domain, the SPP can exist for both TE and TM polarizations, if there is no dielectric spacer. Therefore, the direct contact of semiconductor-metallic back reflector without a dielectric spacer is unlikely to lead to a high absorbance, due to severe SP absorption. The effect of metallic absorption and dielectric spacers will be discussed in Sec. V.

V. ABSORPTION ENHANCEMENT FOR TM INCIDENCE WITH A DIELECTRIC SPACER: GRATING ON THE DIELECTRIC-SPACER (GDS) STRUCTURE AND GRATING ON THE SILVER (GS) STRUCTURE

From Sec. IV, it is seen that the absorbance enhancement for TM incidence on 1D gratings without a dielectric spacer is significantly lower than the diffractive enhancement for TE incidence due to metallic absorption. To improve the silicon absorption by reducing metallic absorption, the $J_{SC,LT}$ is now calculated for dielectric-spaced structures for TM incidence, and the geometry optimization is carried out for the grating period (Λ), FF, grating height (hg), incident angle (θ), and dielectric spacer thickness (t_{ds}), as illustrated in Fig. 6. In theoretical papers, there are two types of structure exist for dielectric spaced metallic back reflectors:[33,34] One is GDS[33] and the other is GS.[34] The GDS structure is illustrated on the left in Fig. 6 where the grating is etched on the dielectric spacer and the silver-dielectric spacer interface is mostly flat. The GS structure is illustrated on the right in Fig. 6 where a grating is formed on the silver surface and then a conformal dielectric spacer layer is deposited on silver. In experiment, GS structure is mostly conducted, and the practice is texturing the silver back reflector before depositing the subsequent layers. Therefore, the experimental structure is more similar to the GS structure. Nonetheless, it is going to be shown that the GS structure is less efficient then the GDS structure at their respective optimized geometry, due to the lower metallic absorption of the GDS structure. For GDS structure, the optimized geometry is $\Lambda = 0.67\,\mu$m, FF $= 0.44$, hg $= 0.15\,\mu$m, $t_{ds} = 0.05\,\mu$m, and $\theta = 4.25°$. For GS structure, the optimized geometry is $\Lambda = 0.64\,\mu$m, FF $= 0.26$, hg $= 0.09\,\mu$m, $t_{ds} = 0.2\,\mu$m, and $\theta = 4.41°$. t_{front} is fixed at 80 nm for both structures. The optimized highest short circuit current at light trapping wavelength, $J_{SC,LT}$, is 6.79 mA/cm^2 for the GDS structure, and 5.99 mA/cm^2 for the GS structure, which are all higher than the case without the dielectric spacer for TM incidence in Sec. IV ($J_{SC,LT} = 4.77$ mA/cm^2). The improvement in $J_{SC,LT}$ for GDS structure is 42.35%, compared to the case without a dielectric spacer in Sec. IV.

It should be pointed out that the number of excited quasi-guided modes also shows increase as the optimization proceeds, but the optimization still does not converge to the geometry that leads to the most supported modes. In order to keep the paper concise, the statistics for the optimization is not shown here again for the dielectric-spaced structures. Repeated global optimization runs are also conducted, and similar results are arrived. Therefore, the optimized geometry giving the highest short circuit current does not coincide with the geometry leading to the most quasi-guided modes. With the dielectric spacer, the metallic absorption is effectively reduced and the optimized trade-off between SP excitation and SP absorption leads to higher silicon absorbance. Therefore, for the plasmonic structures in inorganic solar cells, direct contact of metal-semiconductor, such as the case in Sec. IV, tends to result in increased metallic absorption and is not a preferable way for light trapping. While near field SP effect can be extremely effective[2,10] in organic devices, the far field SP light scattering by metallic back reflectors in inorganic semiconductor can be significantly degraded by metallic absorption. The metallic loss is especially detrimental if a whole metallic back reflector is

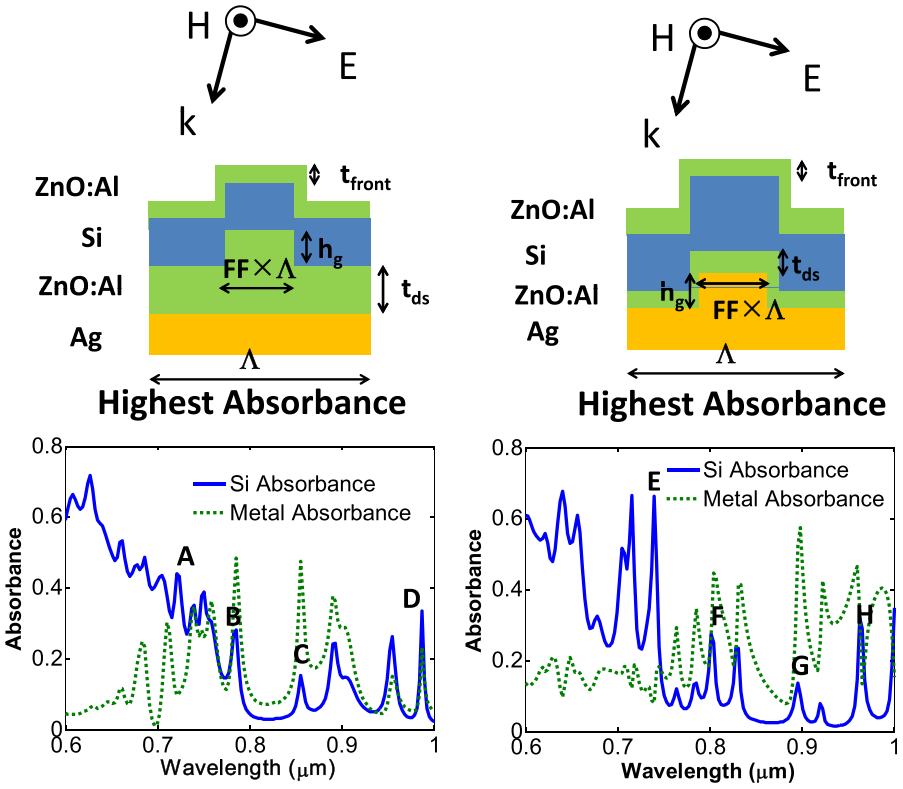

FIG. 6. The highest short circuit current spectral response for the dielectric-spaced metallic back reflectors after optimization for (left) the GDS structure and (right) the GS structure.

directly in contact with the semiconductor,[1] compared to the case where only small nano-scale metallic particles are placed at the front or the rear side of the devices.[35] While a lot of plasmonic structures possesses metal back reflectors directly in contact with inorganic semiconductor is conducted,[1,5] it is suggested here that the conventional dielectric spaced back reflector is still more efficient for long-wavelength light trapping, due to the balance between SP assisted absorption enhancement and metallic absorption loss. Surprisingly, it is also found that the GDS itself is more effective than the GS back reflector, different from the experimental practice were the metallic back reflectors are textured before the subsequent depositions. The higher $J_{SC,LT}$ is mainly because the GS structure tends to lead to more metallic absorption, evident from the spectral response in Fig. 6.

Since in reality the two-dimensional texture or grating is mostly used for solar cells, the excitation of surface plasmon exists for both TE and TM polarizations, if there is no dielectric spacer. It is therefore suggested that for solar cells with metal back reflectors, dielectric spacer should be included and the texture should be formed on the dielectric spacer itself to maximize short circuit current. In the cases where purely diffractive dielectric mirrors are employed, high-Q diffractive modes should be utilized to maximize the short circuit current as evident from Sec. III. In addition, while most of the experimental solar cells still employ metal back reflectors, back reflectors with no SP absorption, such as dielectric mirrors, can potentially provide higher photocurrent due to lower SP absorption loss based on the comparison in this work.

Figs. 7 and 8 show the field profiles and the photonic bandstructures of the optimized geometry, for both GDS and GS dielectric-spaced structures. It can be seen from Fig. 6 that in spectral responses some of the quasi-guided mode peaks are accompanied by the elevated metallic absorption, while the other peaks are not. The quasi-guided mode excitation is also labeled in the photonic bandstructures at the right of Figs. 7 and 8. The Bloch wavefunction for a periodic structure can generally be written as

$$\vec{E}(\vec{r},t) = \mathrm{Re}\left\{\vec{u}(\vec{r})\exp(-j\vec{k}_{Bloch}\cdot\vec{r})\exp(j\omega t)\right\}, \quad (3)$$

where E is the electric field, k_{Bloch} is the Bloch wavevector, ω is angular frequency, t is the time, and u is the periodic modulation. The condition for the excitation of the qausi-guided modes is

$$k_0 \sin\theta = \omega\sqrt{\mu_0\varepsilon_0}\sin\theta = \vec{k}_{Bloch}, \quad (4)$$

where k_0 is the free space wavevector of the incident field, μ_0 and ε_0 are the free space permeability and permittivity, respectively, and θ is the incidence angle as illustrated in Fig. 1. It should be pointed out that here the x-axis in the photonic bandstructure is θ rather than k_{Bloch}, and the conversion between them is also established by Eq. (4).

The slope of the photonic band structure is the photon group velocity

$$\frac{d\omega}{dk_{Bloch}} = \frac{d\omega}{d\theta}\left(\frac{dk_{Bloch}}{d\theta}\right)^{-1} = \frac{d\omega}{d\theta}\frac{1}{k_0\cos\theta}. \quad (5)$$

Although the slow light enhancement is not the main point of this paper, it is still worth to point out that at the quasi-guided mode wavelengths, the photon group velocity is significantly slower than its free space phase velocity and therefore the enhanced absorbance can be achieved.

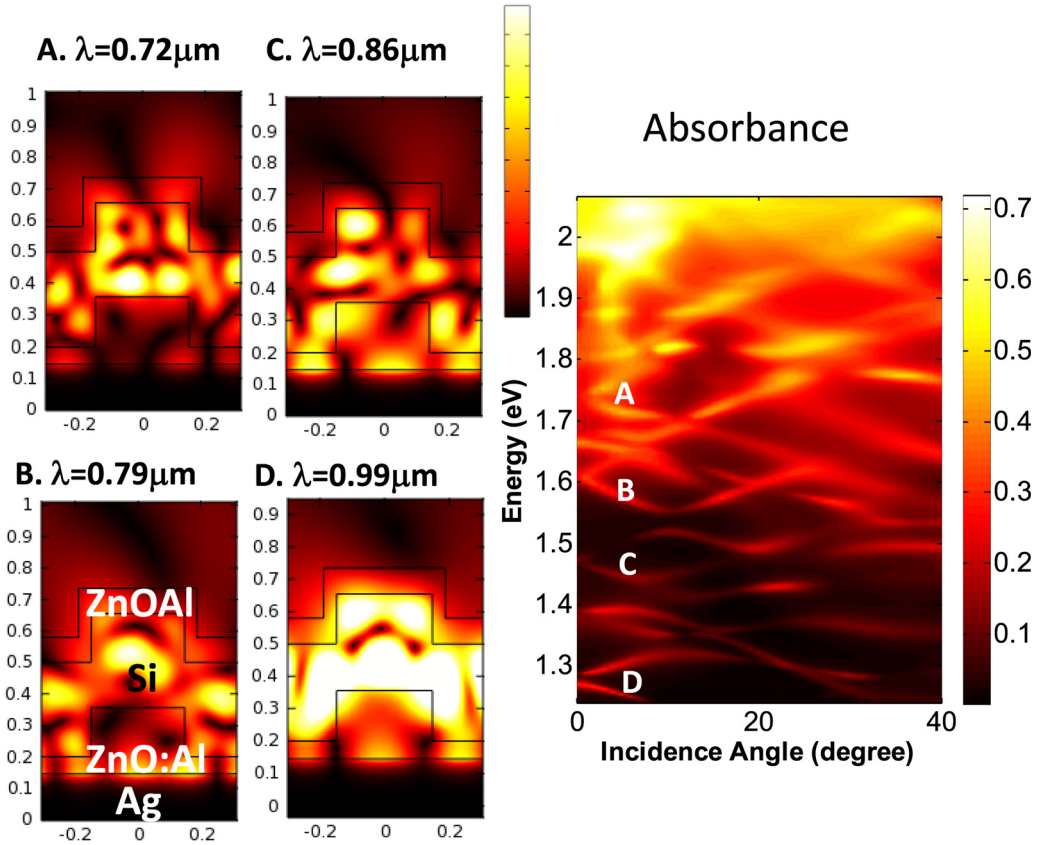

FIG. 7. (Left) The field profiles at the quasi-guided mode peak wavelengths for the optimized GDS structure. (Right) The corresponding photonic bandstructure.

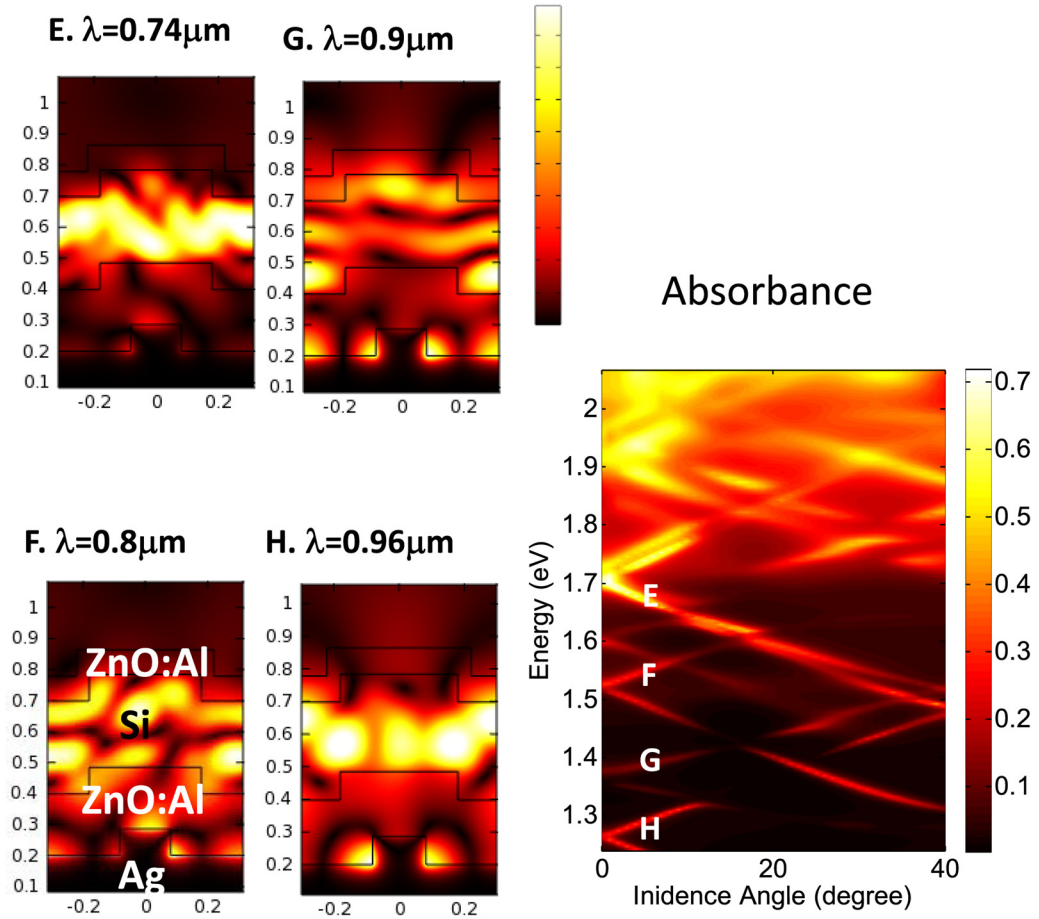

FIG. 8. (Left) The field profiles at the quasi-guided mode peak wavelengths for the optimized GS structure. (Right) The corresponding photonic bandstructure.

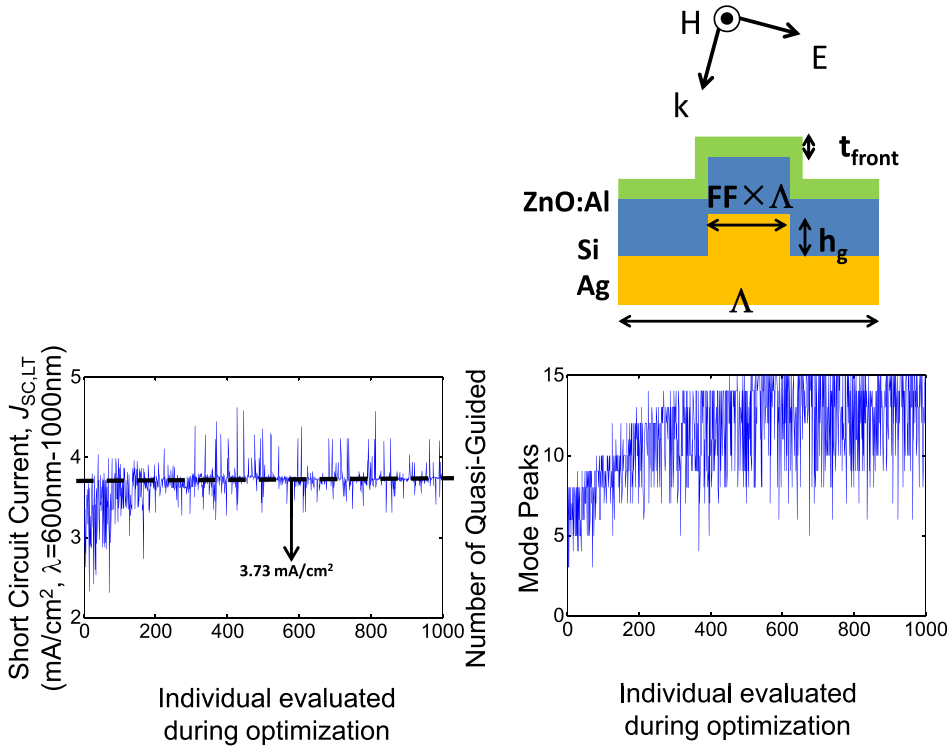

FIG. 9. The statistics of global optimization for TM incidence without a dielectric spacer. The objective function is changed to the number of quasi-guided mode peaks rather than the short circuit current. (Left) Evolution of short circuit current as the optimization proceeds. (Right) Evolution of the number of quasi-guided mode peaks as the optimization proceeds.

VI. ABSORPTION ENHANCEMENT FOR TM INCIDENCE WITHOUT A DIELECTRIC SPACER: OBJECTIVE FUNCTION CHANGED TO THE NUMBER OF QUASI-GUIDED MODE PEAKS

In order to further confirm that the geometry that leads to the most quasi-guide modes does not coincide with the geometry that leads to the highest $J_{SC,LT}$, the objective function of the optimization is now changed to the number of quasi-guided mode peaks rather than the short circuit current used in Secs. III–V. The expected result from the optimization here is to give the geometry whose spectral response shows the largest number of guided modes, and it is interesting to see if the spectral response giving the most modes can lead to very high short circuit current. The optimized geometry is $\Lambda = 0.75\,\mu$m, FF = 0.53, hg = 0.06 μm, and $\theta = 10.08°$; t_{front} is fixed at 80 nm. Fig. 9 again shows the statistics for the optimization run. Now the number of quasi-guided mode peaks increases monotonically during the optimization, but the short circuit current shows an initial increase and then quickly saturates to 3.73 mA/cm^2 with significant overshoots. The $J_{SC,LT} = 3.73$ mA/cm^2 corresponds to the most guided mode geometry, and the overshoots indicate that there exists higher $J_{SC,LT}$ individuals but with fewer supported modes. Fig. 10 shows the corresponding spectral response for the geometry optimized with respect to the number of modes. The total number of quasi-guided mode peaks is around 15, significantly higher than the peak number of the spectral response for the previous study in Sec. IV. Nonetheless, the $J_{SC,LT}$ for the spectral response optimized with respect to the number of modes is only 3.73 mA/cm^2, much lower than the value obtained in Sec. IV ($J_{SC,LT} = 4.77$ mA/cm^2). Therefore, it can be concluded that when using periodic gratings to excite quasi-guided modes to enhance the broad band solar cell absorbance, the number of excited modes is not the solely concern. The resonance strength, the Q-factor, and the guided mode location in the spectrum are all playing critical parts in determining the final short circuit current value.

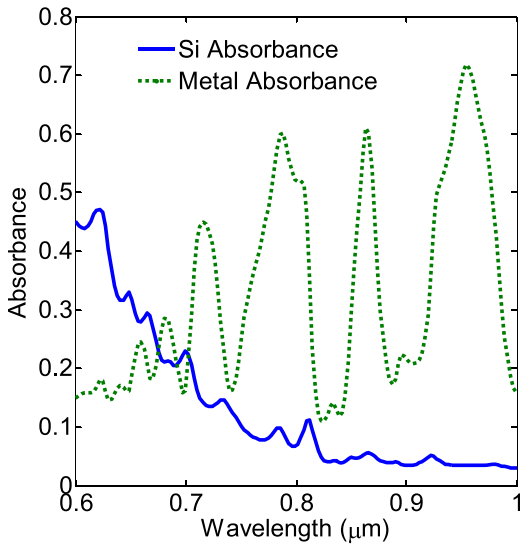

FIG. 10. The optimized spectral absorbance for TM incidence without a dielectric spacer. The objective function is changed to the number of quasi-guided mode peaks rather than the short circuit current at light trapping wavelength.

VII. CONCLUSION

This work shows that although the number of quasi-guided mode peak has a pronounced effect on the solar cell short circuit current, quality factor and the location and the strength of the guided modes also play important roles in determining the final short circuit current value. It is found

that the geometry leading to the most guided modes does not coincide with the geometry leading to the highest short circuit current. For TE incidence, high-Q diffractive peaks are the most efficient way to increase broad band absorbance. On the other hand, for TM incidence on 1D gratings without a dielectric spacer, low-Q modes are always resulted from the global geometry optimization, reflecting the broad band emission nature of surface plasmon photonics. For dielectric-spaced structures, it is surprising that the optimized grating or surface morphology on the dielectric spacer itself is actually more effective for the absorbance enhancement, compared to the optimized grating or morphology on the metallic back reflector. This finding contradicts to most of the experimental practices where the metallic back reflector is textured before the subsequent deposition. With dielectric spacers, $J_{SC,LT}$ can be elevated >40% after proper geometry optimization due to reduced SP absorption. It is suggested for solar cells with metal back reflectors, dielectric spacer is indispensible, and the texture should be formed on the dielectric spacer itself rather than on the metal. In the cases where purely diffractive dielectric mirrors are employed, high-Q modes should be utilized to maximize the short circuit current. Finally, the optimization of the mode quality is proved to be critical in all cases, in addition to the number of supported modes.

ACKNOWLEDGMENTS

This work was funded by National Science Council (NSC), Taiwan, under Grant No. NSC 101-2218-E-009-001.

[1]H.-Y. Lin, Y. Kuo, C.-Y. Liao, C. C. Yang, and Y.-W. Kiang, Opt. Express **20**(S1), A104–A118 (2012).
[2]K. Q. Le, A. Abass, B. Maes, P. Bienstman, and A. Alù, Opt. Express **20**(S1), A39–A50 (2012).
[3]C. Battaglia, C.-M. Hsu, K. S. derstrom, J. Escarre, F.-J. Haug, M. Charriere, M. Boccard, M. Despeisse, D. T. L. Alexander, M. Cantoni, Y. Cui, and C. Ballif, ACS Nano **6**(3), 2790–2797 (2012).
[4]Z. Yu and S. Fan, Appl. Phys. Lett. **98**, 011106 (2011).
[5]U. W. Paetzold, E. Moulin, B. E. Pieters, R. Carius, and U. Rau, Opt. Express **19**(S6), A1219–A1230 (2011).
[6]N. Lagos, M. M. Sigalas, and E. Lidorikis, Appl. Phys. Lett. **99**(6), 063304 (2011).
[7]F. J. Beck, S. Mokkapati, and K. R. Catchpole, Opt. Express **19**(25), 25230–25241 (2011).
[8]Z. Yu, A. Raman, and S. Fan, Opt. Express **18**(S3), A366–A380 (2010).
[9]S. Pillai and M. A. Green, Sol. Energy Mater. Sol. Cells **94**, 1481–1486 (2010).
[10]C. Min, J. Li, G. Veronis, J.-Y. Lee, S. Fan, and P. Peumans, Appl. Phys. Lett. **96**(13), 133302 (2010).
[11]V. E. Ferry, M. A. Verschuuren, H. B. T. Li, E. Verhagen, R. J. Walters, R. E. I. Schropp, H. A. Atwater, and A. Polman, Opt. Express **18**(102), A237–A245 (2010).
[12]H. A. Atwater and A. Polman, Nature Mater. **9**, 205–213 (2010).
[13]A. Lin and J. D. Phillips, Sol. Energy Mater. Sol. Cells **92**, 1689–1696 (2008).
[14]K. R. Catchpole and A. Polman, Opt. Express **16**(26), 21793–21800 (2008).
[15]Z. Yu, A. Raman, and S. Fan, Proc. Natl. Acad. Sci. U.S.A. **107**(41), 17491–17496 (2010).
[16]D. E. Goldberg, *Genetic Algorithms in Search, Optimization, and Machine Learning*, 1st ed. (Addison-Wesley Professional, 1989).
[17]COMSOL AB, Comsol Multiphysics RF Module User Guide, version 3.3, 2006.
[18]C. Haase and H. Stiebig, Prog. Photovoltaics **14**, 629–641 (2006).
[19]P. Bhattacharya, *Semiconductor Optoelectronic Devices*, 2nd ed. (Prentice-Hall, Upper Saddle River, NJ, 2006).
[20]Synopsys, Sentaurus Device User Guide, Version X-2005.10, 2005.
[21]B. Deken, S. Pekarek, and F. Dogan, Comput. Mater. Sci. **37**, 401–409 (2006).
[22]S. Preblea, M. Lipson, and H. Lipson, Appl. Phys. Lett. **86**, 061111–061113 (2005).
[23]L. Shen, Z. Ye, and S. He, Phys. Rev. B **68**, 035109 (2003).
[24]H. Lipson and J. B. Pollack, Nature **406**, 974–978 (2000).
[25]M. Yang, Z. Fu, F. Lin, and X. Zhu, Opt. Express **19**(S4), A763–A771 (2011).
[26]Rsoft, *Rsoft CAD User Manual*, 8.2 ed. (Rsoft Design Group, New York, 2010).
[27]M. E. Fragala, G. Malandrino, M. M. Giangregorio, M. Losurdo, G. Bruno, S. Lettieri, L. S. Amato, and P. Maddalena, Chem. Vap. Deposition **15**, 327–333 (2009).
[28]J. W. Elam, D. Routkevitch, and S. M. George, J. Electrochem. Soc. **150**(6), G339–G347 (2003).
[29]H. Kim, A. Pique, J. S. Horwitz, H. Murata, Z. H. Kafafi, C. M. Gilmore, and D. B. Chrisey, Thin Solid Films **377–378**, 798–802 (2000).
[30]J. M. Khoshman and M. E. Kordesch, Thin Solid Films **515**, 7393–7399 (2007).
[31]C. Munuera, J. Zuniga-Perez, J. F. Rommeluere, V. Sallet, R. Triboulet, F. Soria, V. Munoz-Sanjose, and C. Ocal, J. Cryst. Growth **264**, 70–78 (2004).
[32]V. Shah, H. Schade, M. Vanecek, J. Meier, E. V.-S. ain, N. Wyrsch, U. Kroll, C. Droz, and J. Bailat, Prog. Photovoltaics **12**, 113–142 (2004).
[33]X. Sheng, S. G. Johnson, J. Michel, and L. C. Kimerling, Opt. Express **19**(S4), A841–A850 (2011).
[34]K. Söderström, F.-J. Haug, J. Escarré, O. Cubero, and C. Ballif, Appl. Phys. Lett. **96**(21), 213508 (2010).
[35]S. Pillai, F. J. Beck, K. R. Catchpole, Z. Ouyang, and M. A. Green, J. Appl. Phys. **109**, 073105 (2011).